Correlated Ions in a Calcium Channel Model: A Poisson–Fermi Theory

2 AUTHORS:

Jinn-Liang Liu
National Hsinchu University of Education
68 PUBLICATIONS   **474** CITATIONS

SEE PROFILE

Robert Eisenberg
Rush University Medical Center
297 PUBLICATIONS   **7,629** CITATIONS

SEE PROFILE

# Correlated Ions in a Calcium Channel Model: A Poisson−Fermi Theory

Jinn-Liang Liu

Department of Applied Mathematics, National Hsinchu University of Education, Hsinchu 300, Taiwan

Bob Eisenberg*

Department of Molecular Biophysics and Physiology, Rush University, 1653 West Congress Parkway, Chicago, Illinois 60612, United States

ABSTRACT: We derive a continuum model, called the Poisson−Fermi equation, of biological calcium channels (of cardiac muscle, for example) designed to deal with crowded systems in which ionic species and side chains nearly fill space. The model is evaluated in three dimensions. It includes steric and correlation effects and is derived from classical hard-sphere lattice models of configurational entropy of finite size ions and solvent molecules. The maximum allowable close packing (saturation) condition is satisfied by all ionic species with different sizes and valences in a channel system, as shown theoretically and numerically. Unphysical overcrowding ("divergence") predicted by the Gouy−Chapman diffuse model (produced by a Boltzmann distribution of point charges with large potentials) does not occur with the Fermi-like distribution. Using probability theory, we also provide an analytical description of the implicit dielectric model of ionic solutions that gives rise to a global and a local formula for the chemical potential. In this primitive model, ions are treated as hard spheres and solvent molecules are described as a dielectric medium. The Poisson−Fermi equation is a local formula dealing with different correlations at different places. The correlation effects are apparent in our numerical results. Our results show variations of dielectric permittivity from bath to channel pore described by a new dielectric function derived as an output from the Poisson−Fermi analysis. The results are consistent with existing theoretical and experimental results. The binding curve of Poisson−Fermi is shown to match Monte Carlo data and illustrates the anomalous mole fraction effect of calcium channels, an effective blockage of permeation of sodium ions by a tiny concentration (or number) of calcium ions.

Ca^{2+} and Na^+ in a Channel

Poisson Fermi Equation

$$\varepsilon_w(l_c^2\nabla^2 - 1)\nabla^2\varphi = \sum_{i=1}^{K} q_i C_i = \rho$$
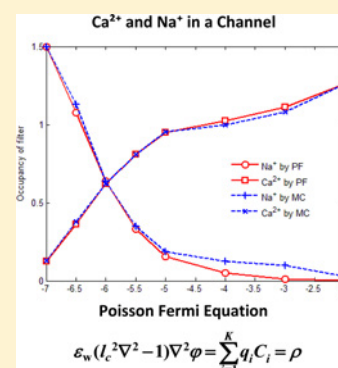
INTRODUCTION

Biological ion channels are protein molecules that span cell membranes and conduct ions through a narrow pore formed by the amino acids and their side chains, some of which may mix with the ions in some types of channels. Ion channels control a wide range of biological functions from signal transfer in the nervous system, coordination of muscle contraction, transport of dissolved substances and water, to regulation of secretion of hormones.[1−3] Each of these functions has been so important for so long that evolution has probably produced a nearly optimal adaptation, within physical constraints, and conserved it, using the same design principles again and again.

Calcium channels are vital to an animal because calcium concentrations (in the range 0.01−1 μM) inside its cells are used as a signal in almost all its tissues in the same sense that the position of a gas pedal is a signal that controls the speed of a car. Calcium channels preferentially and exquisitely conduct Ca^{2+} compared to monovalent cations and exhibit the anomalous mole fraction effect that effectively blocks monovalent cations by a small concentration of Ca^{2+}.[4] For example, the L-type calcium channel has a Ca^{2+} affinity of 1 μM. In 30 mM Na^+, as little as 1 μM Ca^{2+} reduces the Na^+ current measured in 0 Ca^{2+} by 50%.[5,6] Calcium channels also discriminate between ions with the same charge (e.g., Ca^{2+} vs Ba^{2+} or Na^+ vs K^+).[7,84]

The theory that best describes experimental properties of calcium channels is charge/space competition in the crowded charge mechanism introduced by Nonner and Eisenberg to describe the selectivity filter of calcium channels. This theory produces micromolar Ca^{2+} affinity for the L-type calcium channel,[9−12] describes how different calcium channel subclasses can have the wide range of Ca^{2+} affinities seen in experiments,[11,13,14] correctly distinguishes between monovalent cations of different size,[15−17] and uses the same small set of adjustable parameters—channel diameter and one or two dielectric coefficients—to account for the main selectivity properties of calcium and sodium channels.[10,11,15,18−21] Gillespie's treatment of the ryanodine receptor is in the same spirit and is even more successful. Gillespie's treatment accounts for and predicts current voltage relations in a range

of solutions, including quantitatively predicting anomalous mole fraction effects that were not anticipated (by the experimental community) before they were measured.[17,22−25]

Reduced models[9,10,12,15,26] of the calcium channel have been used to develop the charge/space competition theory. In these models, the side chains of proteins are treated as spherical structural $O^{1/2−}$ ions confined to but movable in the filter that interact with mobile ions Na^+, Ca^{2+}, and $Cl^−$ through volume exclusion and electrostatics much as the mobile ions interact with each other. The ions and side chains thus mingle together in the selectivity filter of the channel. That geometry is simply taken to be a doughnut shape, as shown in the cross-sectional view in Figure 1, where H and R denote the length and radius
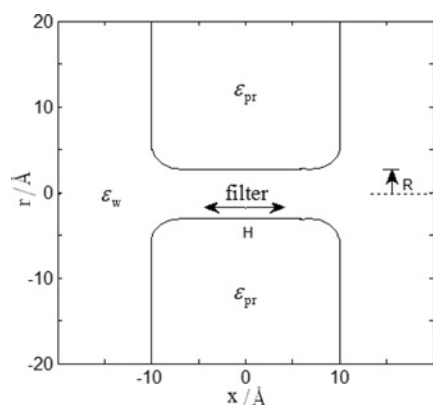

Figure 1. A cross section of the cylindrical shaped channel model. The length and radius of the filter are H and R, respectively.

of the filter, respectively. The solvent and protein are represented implicitly as dielectrics with the dielectric coefficients ε_w and ε_{pr}, respectively. The solvent domain consists of two baths and the channel pore which contains the filter.

It is obvious, and was apparent to Nonner and Eisenberg from the beginning that these simplified models are a gross oversimplification of the real structure. The reduced model was originally designed to deal with measurements in a broad range of ionic mixtures needed to make the inverse problem of identification of parameters well posed.[26] Since then, many structures of transporters and channels have been measured, but understanding of selectivity and permeation has not been an automatic result in a broad range of ionic mixtures, as measured experimentally. Difficulties in dealing with channels bathed in mixtures should come as no surprise, since mixtures in bulk solutions (without biological complications) themselves pose difficulty.[27−31] It seems that the reduced models of these channels are at least as successful as reduced models of ionic mixtures in bulk solutions. Reduced models of these channels seem to capture the (free) energies used by evolution to control selectivity and permeation well enough to deal with experimental data and biological reality (as far as they have been tested).

Most of the above theoretical results were obtained by the Monte Carlo approach. A few theoretical results are available from continuum models, such as the energy variational analysis model.[32,33] However, continuum models that can yield results in three dimensions, comparable to those of Monte Carlo, are lacking.

We propose here a continuum model with steric and correlation effects for which the entropic energy functional,

involving different sizes and valences of ionic species, is derived from the hard-sphere lattice gas model in a mean-field approximation.[34,35] A physical decomposition is applied to Coulombic interactions between ions with short, intermediate, and long range components parametrized by the correlation length.[36,37] The resulting model is a fourth-order nonlinear partial differential equation (PDE) called the Poisson−Fermi equation[37] in which the correlation effects are described by the fourth-order term and a Fermi-like distribution. In contrast to the Boltzmann distribution of the classical Poisson−Boltzmann equation, the Fermi distribution in general (and the Poisson−Fermi equation in particular) imposes a saturation condition for all ionic species so that their concentrations are bounded by the close packing of hard spheres. The unphysical divergence of the Boltzmann distribution of crowded point charges at large potentials has been a central problem in physical chemistry for more than 100 years,[38,39] as reviewed in refs 35 and 40−44 and advertised in refs 45 and 46. The purpose of this paper is to show that delicate phenomena such as the anomalous mole fraction effect that occurs inside a calcium channel can indeed be effectively and efficiently studied in three dimensions by the Poisson−Fermi equation as well as by the Monte Carlo method, which is computationally more expensive and restricted to equilibrium. Most experiments and essentially all biological function involves flow, away from equilibrium.

Variable dielectric permittivity is a new feature provided as an output by the Poisson−Fermi equation. The variations of dielectric permittivity play an important role in the mechanism of permeating ions through channels. Two major effects are the change in strength of pairwise ionic interactions and the transition from aqueous hydration to channel solvation for an ion as it enters the pore from the bath.

The details of dielectric interactions can determine qualitative properties of the crowded charge, as shown in Figures 8−10 of ref 19. The presence of a dielectric region changes the sodium vs potassium selectivity of a sodium channel model in a crucial way. It is important to get the spatial dependence of the dielectric right: a wide range of engineering devices can be made by spatial variation of ONLY the dielectric coefficient.[47,48] It is possible that evolution, as well as engineers, have used this mechanism, e.g., to create large ion selectivity in potassium channels.[49] So far, this spatial dependence of the dielectric can only be dealt with in a continuum treatment.[50] The dielectric function resulting from the Poisson−Fermi equation may provide a more reliable polarizable force field for more accurate calculations of ion conductance and selectivity than that of the Poisson−Boltzmann equation for which the dielectric permittivity is usually treated as a piecewise constant.

■ MODEL

Poisson−Fermi Equation. Using the hard-sphere lattice gas model in mean-field approximation,[35] the free energy for an aqueous electrolytic system is

$$F = \phi \sum_{j=1}^{K} q_j N_j - k_B T \ln W \tag{1}$$

where ϕ is the electrostatic potential, N_j is the total number of j species ions carrying the charge $q_j = z_j e$ with the valence z_j, k_B is the Boltzmann constant, T is the absolute temperature, and K is the total number of ionic species. The last term describes the entropy of the distribution of all ions and water molecules over a total of N available sites in a system with

$$W = \prod_{j=1}^{K} W_j = \frac{N!}{(\Pi_{j=1}N_j!)(N - \sum_{j=1}^{K} N_j)!} \tag{2}$$

$W_1 = N!/(N_1!(N - N_1)!)$ the number of combinations for the distribution of N_1 in all vacant sites N, $W_2 = (N - N_1)!/(N_2!(N - N_1 - N_2)!)$ for the distribution of N_2 in $N - N_1$ vacant sites after N_1 being distributed, and so on. After all the ions are distributed, there are $N - \sum_{j=1}^{K} N_j = N_{K+1}$ sites that will be filled by water molecules, the last species $K + 1$ of particles in the system. Using the Stirling formula, $\ln M! \approx M \ln M - M$ with $M \gg 1$, for the mixing entropy,[31,48] the chemical potential of ionic species i is

$$\mu_i = \frac{\partial F}{\partial N_i} = q_i \phi + k_B T \ln \frac{N_i}{N - \sum_{j=1}^{K} N_j} \tag{3}$$

from which we deduce global probabilities $p_i = N_i/N$ for all ionic species and $p_{K+1} = 1 - \sum_{j=1}^{K} p_j$ for the molecules of water. By introducing local probabilities $p_i(\mathbf{r}) = v_i C_i(\mathbf{r})$, the chemical potential can be written as a local function

$$\mu_i = q_i \phi(\mathbf{r}) + k_B T \ln \frac{v_i C_i(\mathbf{r})}{1 - \sum_{j=1}^{K} v_j C_j(\mathbf{r})} \quad \text{for}$$

$$i = 1, ..., K \tag{4}$$

where $C_i(\mathbf{r})$ is the concentration function of spatial variable $\mathbf{r}$ in the box domain shown in Figure 1 and $v_i = 4\pi a_i^3/3$ is the volume of each individual ion of species i with a_i being the radius. The volume of the site occupied by this ion is also v_i; i.e., a site is a sphere and its volume changes with different species of resident ions. The denominator indicates that the quantity $\gamma = 1 - \sum_{j=1}^{K} v_j C_j(\mathbf{r}) = v_{K+1} C_{K+1}(\mathbf{r})$ is the volume fraction occupied by—or the local probability of—water molecules in any unit volume. We treat the volume fraction γ as a single entity without specifying the volume v_{K+1} of individual water molecules and the water density C_{K+1}. Therefore, γ represents the continuum solvent surrounding ionic hard-sphere particles in the unit volume. Globally, the N_{K+1} sites of water molecules lump all water molecules into a continuum dielectric background. Equivalently, N_{K+1} sites correspond to the global volume fraction (global probability) of water molecules in the system. A single global volume fraction of water molecules is equivalent to a local distribution of N_{K+1} water molecules, as we now show. The number of combinations for distributing N_{K+1} water molecules in the remaining sites $N - \sum_{j=1}^{K} N_j$ is

$$W_{K+1} = \frac{(N - \sum_{j=1}^{K} N_j)!}{N_{K+1}!(N - \sum_{j=1}^{K+1} N_j)!} = \frac{N_{K+1}!}{N_{K+1}!0!} = 1 \tag{5}$$

which is exactly the number of combinations for distributing a single lumped water in the global volume fraction because

$$W_{K+1} = \frac{1!}{1!0!} = 1 \tag{6}$$

Consequently, the local free energy or chemical potential of any ionic species depends on its local entropy (the numerator in eq 4) and also on the local entropy of water molecules (the denominator). And all water molecules are seen by each ion as a continuum (global) dielectric.

Our derivation from eqs 1, 2, 5, and 6 to the global chemical potential 3 and the local chemical potential 4 can therefore be considered as a mathematical description of the primitive

model of electrolytes, which is used in most Monte Carlo simulations of the L-type calcium channel and plays a key role in density functional theory (DFT) and DFT-PNP (Poisson–Nernst–Planck) models as well.

For a fixed total volume and a fixed temperature of the system, the chemical potential is found to be $\mu_i = k_B T \ln(v_i C_i^B/(1 - \sum_{j=1}^{K} v_j C_j^B))$ by setting $\phi = 0$, where C_i^B denotes the bulk concentration. Consequently, the concentration can be expressed by

$$C_i = \frac{C_i^B \exp(-\beta_i \varphi)}{1 - \sum_{j=1}^{K} v_j C_j^B}(1 - \sum_{j=1}^{K} v_j C_j) = C_i^B \exp(-\beta_i \varphi + S_{trc}) \tag{7}$$

where $\beta_i = q_i/k_B T$ and $S_{trc} = \ln[(1 - \sum_{j=1}^{K} v_j C_j)/(1 - \sum_{j=1}^{K} v_j C_j^B)]$ is called the steric functional, which represents an excess potential—different for each ionic species—beyond that of the ideal dilute solution. Note that the concentration of each species depends on the excess steric potential which in turn depends on the concentration of all species. "Everything" interacts with everything else in crowded systems like this. Interactions are produced by crowding of the ions themselves, crowding of ions and side chains of the protein, as well as allosteric properties and conformation changes of the surrounding protein.

At large potentials such that $-\beta_i \phi \gg 1$, we have

$$\lim_{-\beta_i \phi \to \infty} C_i = \lim_{\alpha_i \to \infty} \frac{\alpha_i - \sum_{j \neq i}^{K} v_j C_j}{1 + v_i \alpha_i} = \frac{1}{v_i} \tag{8}$$

with $\alpha_i = C_i^B \exp(-\beta_i \phi)/(1 - \sum_{j=1}^{K} v_j C_j^B)$; i.e., the concentration cannot exceed the maximum value $1/v_i$. This means that the density distributions (eq 7) are not of the Boltzmann type but rather of the Fermi type, since these distributions have been arranged in the finite N sites. These distributions reduce to Boltzmann if $v_i = S_{trc} = 0$. This limit cannot be reached physically, however, because it would lead to an infinite concentration if $-\beta_i \phi \to \infty$. This fact was known to Stern[51] in 1924.

The development of analytical formulas like eq 7 is quite recent.[35–37,52,53] Formula 7 is more general than the previous formulations, since it permits any number of ionic species with different valences and sizes in a system. A formula of this generality is needed to deal with biological reality, since biological solutions nearly always include a large number of ionic species (as essential ingredients) that are important for biological function and have a wide range of valences and sizes. Interactions between many of these biological species are an important determinant of the properties of channels and enzymes and have been the subject of a large part of experimental work in physiology and biochemistry, for more than 75 years.

We use the Poisson–Fermi equation to describe correlation effects

$$\varepsilon_w(l_c^2 \nabla^2 - 1)\nabla^2 \phi = \sum_{i=1}^{K} q_i C_i = \rho \tag{9}$$

proposed in refs 36 and 37, where l_c is an electrostatic correlation length and $\hat{\varepsilon} = \varepsilon_w(1 - l_c^2 \nabla^2)$ is a dielectric operator that approximates the permittivity of the surrounding material and the linear response of correlated ions.[37,53] The ionic interaction potential described by eq 9 is a mean field due to

continuous charge density ρ, which is in contrast to the mean force employed by the Monte Carlo treatment primitive implicit dielectric model of ions in solutions and channels.

This equation reduces to the Poisson–Boltzmann equation when $l_c = 0$. The correlation length l_c determines not only the strength of correlations[37] but also the boundary between the short and long range Coulombic interactions of all ionic particles involved in the system.[36] These physical properties, generally inexplicable by the standard second-order Poisson–Boltzmann equation,[45,46] can be used to study sensitive phenomena such as the interplay between overscreening from short range correlations and crowding from finite size effects at large potentials.[37] Apart from the Poisson–Fermi approach, the density functional (continuum) description of ion–ion, ion–solute, or ion–water Lennard-Jones interactions has been independently proposed and studied by our group[32,33] and by Wei's group[54] in recent years to deal with steric and correlation effects.

The fourth-order eq 9 is reduced to a second-order PDE in ref 55

$$
\begin{cases}
\varepsilon_w(l_c^2\nabla^2 - 1)\Psi = \rho \\
\nabla^2\phi = \Psi
\end{cases}
\tag{10}
$$

by introducing an additional unknown function Ψ with suitable boundary conditions. Numerical methods to solve these equations in three dimensions are developed in ref 55.

Dielectric Function. The solvent in an electrolyte is represented by a dielectric constant in classical Poisson–Boltzmann theory as in other primitive implicit dielectric models of ionic solutions. In the Poisson–Fermi equation (eq 9), the dielectric coefficient $\hat{\varepsilon} = \varepsilon_w(1 - l_c^2\nabla^2)$ is an operator if the correlation length $l_c \neq 0$. The operator is not a scalar and cannot directly yield a single dielectric quantity. From eq 10, the image of the function $\Psi(\mathbf{r})$ under the operator $\hat{\varepsilon}$ is the scalar function $\rho(\mathbf{r})$. If $l_c = 0$, then $\hat{\varepsilon} = \varepsilon_w$, which is not an operator but indeed a scalar, the dielectric constant of bulk water. Thus, there exists an unknown dielectric function, say $\tilde{\varepsilon}(\mathbf{r})$, that is implicitly defined by the operator $\hat{\varepsilon}$ when $l_c \neq 0$. We now derive a computable formula for $\tilde{\varepsilon}(\mathbf{r})$.

The polarization $\mathbf{P}$ of the solvent induced by the electric field $\mathbf{E} = -\nabla\phi$ is described by the Poisson equation[54]

$$
\varepsilon_w \nabla \cdot \mathbf{E} = \rho - \nabla \cdot \mathbf{P}
\tag{11}
$$

where the polarization charge density $\eta = -\nabla \cdot \mathbf{P} = -\varepsilon_w\Psi - \rho$ can be calculated, since the function $\Psi = -\nabla \cdot \mathbf{E}$ and the charge density ρ have been obtained by solving eq 10. Equation 11 means that the total charge density $\rho(\mathbf{r})$ of ions is equal to the density $\rho_w(\mathbf{r}) = \varepsilon_w\nabla \cdot \mathbf{E} = -\varepsilon_w\nabla^2\phi(\mathbf{r})$ minus the polarization charge density $\eta(\mathbf{r})$.

In a uniform homogeneous medium, the density function $\rho_w(\mathbf{r})$ is a continuous distribution function of all ions interacting whose dielectric permittivity is a single constant ε_w over the solvent domain. Where the solvent is not a uniform dielectric, the polarization charge density $\eta(\mathbf{r})$ is induced in the solvent by the electric field $\mathbf{E}$, giving the varying dielectric $\tilde{\varepsilon}(\mathbf{r})$. Note that this polarization charge is in the solvent, not on the surface of protein.

Assuming that the electrolyte is isotropic, $\tilde{\varepsilon}(\mathbf{r})$ then satisfies the Poisson equation $\nabla \cdot \tilde{\varepsilon}\mathbf{E} = \rho$. By the approximation $\nabla \cdot \tilde{\varepsilon}\mathbf{E} \approx -\tilde{\varepsilon}\Psi$ and $\eta = -\varepsilon_w\Psi - \rho$, we then have the computable dielectric function

$$
\tilde{\varepsilon}(\mathbf{r}) \approx \frac{\varepsilon_w}{1 + \eta(\mathbf{r})/\rho(\mathbf{r})}
\tag{12}
$$

Chemical Potentials in the Filter. In the baths, the bulk concentration C_i^B for each species i is related to its chemical potential by

$$
\mu_i = k_B T \ln[v_i C_i^B / (1 - \sum_{j=1} v_j C_j^B)]
\tag{13}
$$

However, in the filter region, the bulk value C_i^F is not known and is not equal to C_i^B because we have additional oxygen ions. An extra potential V_c is devised to keep these structural ions in the filter, namely, $C_4 = C_4^F \exp(-\beta_4\phi + S_{trc} + V_c)$ instead of eq 7. Here, V_c is chosen to be the hard-wall confinement potential[20] and ionic species Na^+, Ca^{2+}, Cl^-, and $O^{1/2-}$ are enumerated by $i = 1, 2, 3$, and 4, respectively. The confinement potential and C_4^F are implicitly and self-consistently determined by constraining the total number of $O^{1/2-}$ to 8 at each Newton's iteration. If the water volume fraction $\gamma^F = 1 - \sum_{j=1} v_j C_j^F$ is fixed in the filter, the values of C_j^F are also fixed; i.e., the remaining volume available to permeable ions is fixed. Neglecting C_3^F since chloride ions are completely depleted in the filter region by $O^{1/2-}$ ions, we have

$$
\mu_i^F = k_B T \ln(v_i C_i^F / \gamma^F), \quad i = 1, 2
\tag{14}
$$

which thus establishes a relationship between C_i^F and μ_i^F. The filter chemical potential μ_i^F is one of the two tuning parameters used to match the Monte Carlo results in ref 20, while the correlation length l_c is the other one. We are aware that leaving out co-ions altogether may be too drastic an approximation and we intend to be less drastic in future work: trace concentrations of minority carriers (another name for co-ions) have long been known to be important in semiconductor devices[56,57] and ion exchangers.[58]

Instead of using ion activity in eq 13, we use the concentration because it can be directly evaluated in eq 7. Otherwise, the activity coefficient (defined by the relationship between activity and concentration) would need to be additionally determined in the variable ionic conditions that change so much between the baths and the selectivity filter of channels. Note that, for the case $v_i = 0$ (reducing to Poisson–Boltzmann), eq 13 should be written as $\mu_i = k_B T \ln[C_i^B/C_{K+1}^B]$, since the denominator is $v_{K+1}C_{K+1}^B$ and the ratio v_i/v_{K+1} is a constant before taking all particle volumes v_j, $j = 1, ..., K + 1$, to the limiting zero. For eq 7, this limiting reduction to the Boltzmann distribution is still valid provided that the water density is assumed to be constant in the entire solvent domain.

■ RESULTS

We first study the concentration profiles produced by Poisson–Fermi for the case of $[CaCl_2] = 10^{-6}$ M and $[NaCl] = 30$ mM. The parameter values $R = 3.5$ Å, $H = 10$ Å, $a_1 = a_{Na^+} = 0.95$ Å, $a_2 = a_{Ca^{2+}} = 0.99$ Å, $a_3 = a_{Cl^-} = 1.81$ Å, $a_4 = a_{O^{1/2-}} = 1.4$ Å, $\varepsilon_w = 80$, and $\varepsilon_{pr} = 10$ in ref 20 are used here to compare with Monte Carlo results. The oxygen ions $O^{1/2-}$ are confined in the filter region by the hard-wall confining potential defined in ref 20 and illustrated in Figure 2. The $O^{1/2-}$ profile obtained by Poisson–Boltzmann (without S_{trc}) is shown by a dotted curve and by Poisson–Fermi by a solid curve. From eq 8, the steric functional S_{trc} imposes a saturation condition on the oxygen ions in the filter; namely, the following inequality
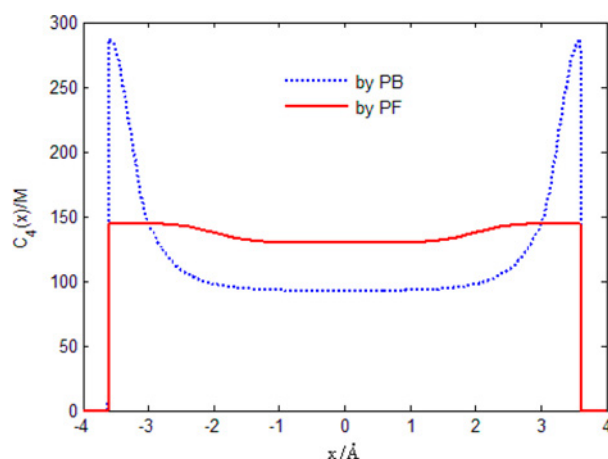
Figure 2. The concentration profiles $C_4(\mathbf{r})$ of oxygen ions $O^{1/2-}$ by Poisson−Boltzmann (PB) in dotted curve and by Poisson−Fermi (PF) in solid curve.

$$C_4(\mathbf{r}) \leq \frac{1}{\nu_4} = \frac{3}{4\pi a_4^3} = 144.475 \text{ M} \tag{15}$$

holds for the $O^{1/2-}$ concentration function $C_4(\mathbf{r})$ at all points $\mathbf{r}$ in the domain. Ionic solutions with concentration greater than 144.475 M are impossible. At a concentration of $1/\nu_4$, the space of ν_4 is a solid filled with charges.

The Poisson−Fermi equation with the steric functional satisfies the saturation condition due to the Fermi distribution property, whereas the Poisson−Boltzmann equation without finite size effects fails to meet this condition near the walls (at $x = \pm 3.6$ Å) of the confinement region, as shown in Figure 2. This example clearly demonstrates the long-standing problem of unphysically high concentration of ionic particles near boundaries with large potentials predicted by the Gouy−Chapman diffuse model. The problem arises because the model does not consider steric effects. It is not surprising that the Poisson−Fermi profile is flat due to the combined effect of the crowded filter space and the saturation condition.

Figures 3 and 4 present Poisson−Boltzmann and Poisson−Fermi profiles for Na^+ and Ca^{2+}. The numbers of Na^+ obtained by Monte Carlo, Poisson−Boltzmann, and Poisson−Fermi are 0.64 (estimated from Figure 8 in ref 19), 0.76, and 0.64, respectively, whereas the corresponding numbers are 0.62, 0.57, and 0.62 for Ca^{2+}. We can match the occupancy estimated by Poisson−Fermi almost exactly to that found by Monte Carlo by tuning the two parameters mentioned above. For this model (eq 7), as for all models of the Nonner−Eisenberg type, the side chains of the channel protein are described by effective values C_1^F and C_2^F. The utility of this class of models in fitting large amounts of data (with a few unvarying parameters) justifies the approach. We determine the values of these constants by adjusting μ_i^F according to formula 14. From Figure 4, we observe that the Poisson−Fermi model (with steric and correlation effects) predicts more Ca^{2+} ions compared to Poisson−Boltzmann (without both effects), since Poisson−Fermi includes finite size effects and Ca^{2+} has a valence advantage competing with Na^+ for the same space. Na^+ and Ca^{2+} ions have nearly the same size.

It is natural to have two peaks for both Na^+ and Ca^{2+} outside the filter, since the filter is modeled as a hard-wall confinement and contains a net charge of $-2.12e$, which requires more cations in the outside region than inside to provide charge
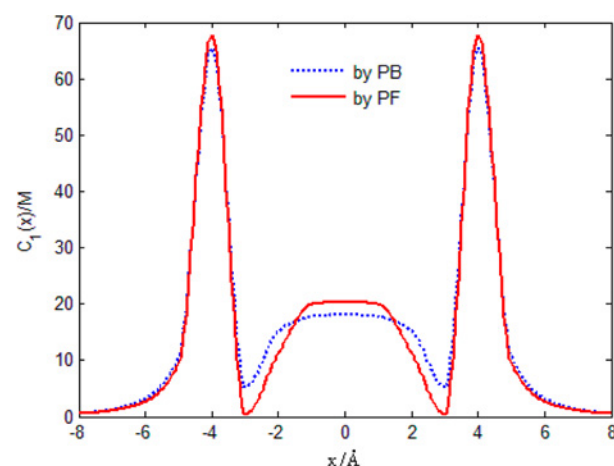

Figure 3. The concentration profiles $C_1(\mathbf{r})$ of sodium ions Na^+ calculated by Poisson−Boltzmann (PB) in dotted curve and by Poisson−Fermi (PF) in solid curve. The corresponding numbers of ions in the filter are 0.76 and 0.64, respectively, with $[CaCl_2] = 10^{-6}$ M and $[NaCl] = 30$ mM.

Figure 4. The concentration profiles $C_2(\mathbf{r})$ of calcium ions Ca^{2+} calculated by Poisson−Boltzmann (PB) in dotted curve and by Poisson−Fermi (PF) in solid curve. The corresponding numbers of ions in the filter are 0.57 and 0.62, respectively, with $[CaCl_2] = 10^{-6}$ M and $[NaCl] = 30$ mM.
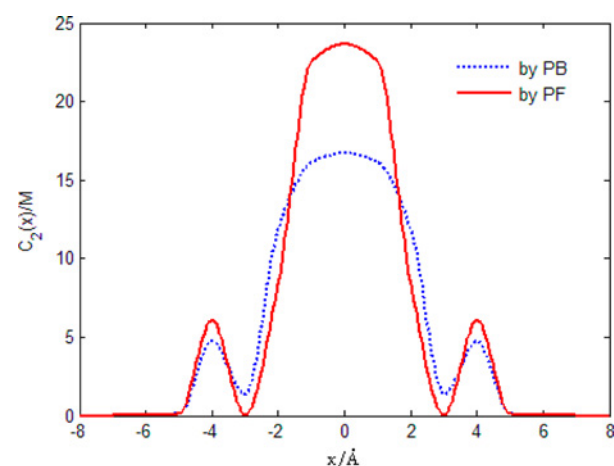
balance for the whole system. The Na^+ peaks are more pronounced, as shown in Figure 3, since $C_1^B = [Na^+] = 30$ mM is much greater than $C_2^B = [Ca^{2+}] = 10^{-6}$ M.

Dielectric Coefficient is an Output. A special feature provided by the Poisson−Fermi equation is its description of spatial variations in the dielectric coefficient of solvent in the channel pore. This important feature must be emphasized because important biological properties of the channel model are known to be sensitive to the treatment of the spatial variation of dielectric coefficient.[18,19] The crucial biological property of sodium vs potassium selectivity is found in a model with a (relatively) high resolution treatment[19] of dielectric regions. Sodium vs potassium selectivity is not found in similar models with fewer dielectric regions.[18]

The dielectric coefficient is an output of our Poisson−Fermi calculations that is affected by the input parameters as described in eq 12 which has a pleasingly simple interpretation. The density of polarization charge and the density of ions of course are also outputs of the calculation. Roughly speaking, the

12055

dx.doi.org/10.1021/jp408330f | J. Phys. Chem. B 2013, 117, 12051−12058

dielectric coefficient varies because the polarization charge density $\eta = -\varepsilon_w \Psi - \rho = \varepsilon_w \nabla \cdot \mathbf{E} - \rho$ varies with the gradient of the electric field $\mathbf{E}$ and the charge density ρ. The averaged dielectric coefficient $\tilde{\varepsilon}(\mathbf{r})$ along the channel axis decreases significantly from its bath value $\varepsilon_w = 80$ to ~42.5 at the center of the channel pore, as shown in Figure 5, which is consistent with well-known theoretical and experimental studies.[59−61]
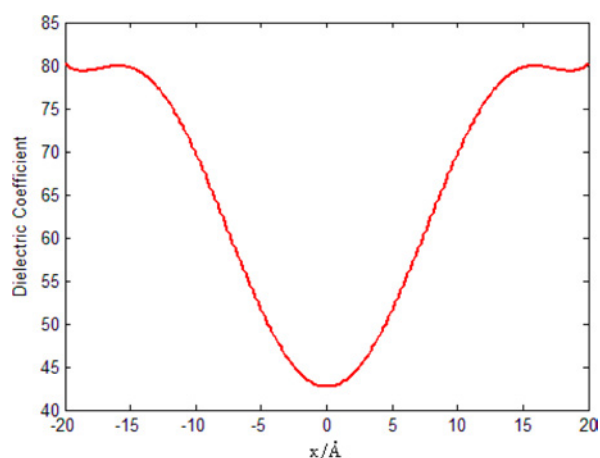

Figure 5. The dielectric profile $\tilde{\varepsilon}(\mathbf{r})$ in the solvent domain obtained by the Poisson−Fermi equation.

For the selectivity of the L-type calcium channel, numerical results obtained by the Poisson−Fermi equation with the correlation length $l_c = 0.577$ Å are in excellent accord with those of Monte Carlo, as shown in Figure 6, which shows that
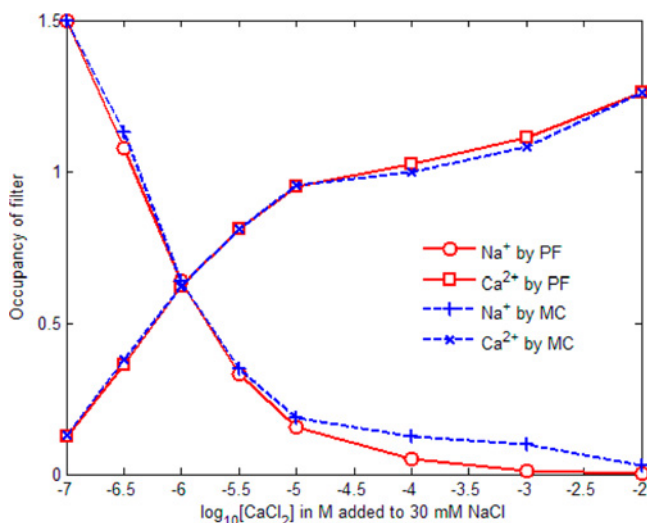

Figure 6. The average number of Ca^{2+} and Na^+ in the selectivity filter varies with increasing $[CaCl_2]$ added to a fixed $[NaCl] = 30$ mM background electrolyte. The MC curve is reproduced from Figure 6c in ref 20.

occupancy of the selectivity filter changes from Na^+ to Ca^{2+} as the concentration $[CaCl_2]$ increases from 10^{-7} to 10^{-2} M at a fixed background electrolyte in the baths with $[NaCl] = 30$ mM. As far as we know, this is the first three-dimensional continuum result that matches Monte Carlo occupancy data almost exactly by tuning only two parameters l_c and μ_i^F.

The correlation length l_c is an effective length scale over which the electrostatic interaction energy is comparable in magnitude to the thermal energy scale.[36,53] Its value is not precisely known[51] and depends primarily on the valences and sizes of all ionic species involved in the system. The adjustment of l_c to fit the Monte Carlo data is arbitrary in the present work. The fitting curve as shown in Figure 6 is not drastically sensitive to this adjustment. However, the value of l_c directly affects the dielectric profile shown in Figure 5, which essentially represents a mean effect of complex physical properties such as correlated interactions, screening, ion size and valence, ionic strength, dipoles and their orientations, and polarization charge density, etc., in the system. Because of this kind of averaging, the ion size is simply taken to be constant throughout the entire domain from bath to pore. The precise size of ions may be crucial for molecular dynamics or Monte Carlo simulations. It does not dramatically affect the mean field approximation, again due to the averaging effect. The overall binding phenomenon as shown in Figure 6 would not change significantly if the radius of oxygen ions were changed from 1.4 Å (ionic radius) to 0.7 Å (covalent radius), since the correlation length can be adjusted. The dielectric profile as an averaged output may be used to validate the Poisson−Fermi equation and its adjustable parameters by comparing with simulation data or even experimental data if that becomes available. The dielectric profile may prove to be an intermediate scale reduced variable more robustly determined by biological data than (for example) ion or channel "diameters". In classical biological language, the dielectric profile may be a phenotype as important as the profile of permanent charge.

From eqs 13 and 14, we observe that the parameter μ_i^F varies with bulk concentrations C_i^B, ion volumes v_i, and the water volume fraction γ in a complex way. The values of μ_2^F are given in Table 1 for various C_2^B. The value of μ_1^F is for $C_1^B = 30$ mM. The water volume fraction $\gamma = 1 - \sum_{j=1}^{K} v_j C_j(\mathbf{r})$ is almost fixed at about $\gamma^F = 0.65$, as required by eq 14.

■ CONCLUSIONS

The Poisson−Fermi equation presented in this paper is a decomposition of Coulombic interactions of correlated ions in the mean-field theory using a hard-sphere lattice gas model for entropic free energy. The Poisson−Fermi equation provides an effective steric functional that modifies classical Poisson−Boltzmann theory to deal with the reality of saturation of concentration, produced by the finite size of ions. The saturation condition is satisfied by all ionic species with various sizes and valences. The saturation condition is of great importance in ion channels, where the number density of ions is very large, often >10 M. The Poisson−Fermi model predicts the anomalous mole fraction effect of real calcium

Table 1. Values of μ_2^F and γ

C_2^B in M	10^{-7}	5×10^{-7}	10^{-6}	5×10^{-6}	10^{-5}	10^{-4}	10^{-3}	10^{-2}
$\mu_2^F/k_B T$	−29.99	−28.25	−26.62	−25.01	−23.32	−21.02	−17.61	−15.31
γ	0.647	0.649	0.651	0.652	0.651	0.652	0.652	0.650

channels. The model also yields a useful formula for the dielectric permittivity as an output of the calculations. The Poisson−Fermi equation can be embedded in the Poisson−Nernst−Planck theory to provide better prediction and description of complex fluids in a great variety of physical, chemical, and biological systems.

■ AUTHOR INFORMATION

Corresponding Author

*E-mail: beisenbe@rush.edu. Phone: +1-312 942 6467. Fax: +1-312942-8711.

Notes

The authors declare no competing financial interest.

■ REFERENCES

(1) Neher, E.; Sakmann, B. Single Channel Currents Recorded from the Membrane of Denervated Muscle Fibers. *Nature* **1976**, *260*, 799−802.

(2) Neher, E. Ion Channels for Communication between and within Cells Nobel Lecture, December 9, 1991. In *Nobel Lectures, Physiology or Medicine 1991−1995*; Ringertz, N., Ed.; World Scientific Publishing Co: Singapore, 1997; pp 10−25.

(3) Sakmann, B.; Neher, E. *Single Channel Recording*, 2nd ed.; Plenum: New York, 1995; p 700.

(4) Sather, W. A.; McCleskey, E. W. Permeation and Selectivity in Calcium Channels. *Annu. Rev. Physiol.* **2003**, *65*, 133−159.

(5) Almers, W.; McCleskey, E. W. Non-Selective Conductance in Calcium Channels of Frog Muscle: Calcium Selectivity in a Single-File Pore. *J. Physiol.* **1984**, *353*, 585−608.

(6) Almers, W.; McCleskey, E. W.; Palade, P. T. Non-Selective Cation Conductance in Frog Muscle Membrane Blocked by Micromolar External Calcium Ions. *J. Physiol.* **1984**, *353*, 565−583.

(7) Hess, P.; Lansman, J. B.; Tsien, R. W. Calcium Channel Selectivity for Divalent and Monovalent Cations. Voltage and Concentration Dependence of Single Channel Current in Ventricular Heart Cells. *J. Gen. Physiol.* **1986**, *88* (3), 293−319.

(8) Hess, P.; Lansman, J. F.; Tsien, R. W. Calcium Channel Selectivity for Divalent and Monovalent Cations. *J. Gen. Physiol.* **1986**, *88*, 293−319.

(9) Nonner, W.; Eisenberg, B. Ion Permeation and Glutamate Residues Linked by Poisson-Nernst-Planck Theory in L-type Calcium Channels. *Biophys. J.* **1998**, *75*, 1287−1305.

(10) Nonner, W.; Gillespie, D.; Henderson, D.; Eisenberg, B. Ion Accumulation in a Biological Calcium Channel: Effects of Solvent and Confining Pressure. *J. Phys. Chem. B* **2001**, *105* (27), 6427−6436.

(11) Boda, D.; Valisko, M.; Eisenberg, B.; Nonner, W.; Henderson, D.; Gillespie, D. The Combined Effect of Pore Radius and Protein Dielectric Coefficient on the Selectivity of a Calcium Channel. *Phys. Rev. Lett.* **2007**, *98*, 168102.

(12) Gillespie, D.; Boda, D. The Anomalous Mole Fraction Effect in Calcium Channels: A Measure of Preferential Selectivity. *Biophys. J.* **2008**, *95* (6), 2658−2672.

(13) Boda, D.; Gillespie, D. Steady-State Electrodiffusion from the Nernst−Planck Equation Coupled to Local Equilibrium Monte Carlo Simulations. *J. Chem. Theory Comput.* **2012**, *8* (3), 824−829.

(14) Kaufman, I.; Luchinsky, D. G.; Tindjong, R.; McClintock, P. V. E.; Eisenberg, R. S. Multi-ion Conduction Bands in a Simple Model of Calcium Ion Channels. *Phys. Biol.* **2013**, *10* (2), 026007.

(15) Boda, D.; Valisko, M.; Henderson, D.; Eisenberg, B.; Gillespie, D.; Nonner, W. Ionic Selectivity in L-type Calcium Channels by Electrostatics and Hard-Core Repulsion. *J. Gen. Physiol.* **2009**, *133* (5), 497−509.

(16) Boda, D.; Henderson, D.; Busath, D. D. Monte Carlo Study of the Effect of Ion and Channel Size on the Selectivity of a Model Calcium Channel. *J. Phys. Chem. B* **2001**, *105* (47), 11574−11577.

(17) Gillespie, D.; Giri, J.; Fill, M. Reinterpreting the Anomalous Mole Fraction Effect. The Ryanodine Receptor Case Study. *Biophys. J.* **2009**, *97* (8), 2212−2221.

(18) Boda, D.; Busath, D.; Eisenberg, B.; Henderson, D.; Nonner, W. Monte Carlo Simulations of Ion Selectivity in a Biological Na+ Channel: Charge-Space Competition. *Phys. Chem. Chem. Phys.* **2002**, *4*, 5154−5160.

(19) Boda, D.; Nonner, W.; Valisko, M.; Henderson, D.; Eisenberg, B.; Gillespie, D. Steric Selectivity in Na Channels Arising from Protein Polarization and Mobile Side Chains. *Biophys. J.* **2007**, *93* (6), 1960−1980.

(20) Malasics, A.; Gillespie, D.; Nonner, W.; Henderson, D.; Eisenberg, B.; Boda, D. Protein Structure and Ionic Selectivity in Calcium Channels: Selectivity Filter Size, not Shape, Matters. *Biochim. Biophys. Acta, Biomembr.* **2009**, *1788* (12), 2471−2480.

(21) Boda, D.; Busath, D. D.; Henderson, D.; Sokolowski, S. Monte Carlo Simulations of the Mechanism of Channel Selectivity: the Competition between Volume Exclusion and Charge Neutrality. *J. Phys. Chem. B* **2000**, *104*, 8903−8910.

(22) Gillespie, D.; Xu, L.; Meissner, G. Selecting Ions by Size in a Calcium Channel: the Ryanodine Receptor Case Study. *Biophys. J.* **2010**, *98* (3, Suppl. 1), 332a.

(23) Krauss, D.; Gillespie, D. Sieving Experiments and Pore Diameter: it's not a Simple Relationship. *Eur. Biophys. J.* **2010**, *39*, 1513−1521.

(24) Krauss, D.; Eisenberg, B.; Gillespie, D. Selectivity Sequences in a Model Calcium Channel: Role of Electrostatic Field Strength. *Eur. Biophys. J.* **2011**, *40* (6), 775−782.

(25) Gillespie, D.; Chen, H.; Fill, M. Is Ryanodine Receptor a Calcium or Magnesium Channel? Roles of K(+) and Mg(2+) during Ca(2+) Release. *Cell Calcium* **2012**, *51* (6), 427−33.

(26) Boda, D.; Nonner, W.; Henderson, D.; Eisenberg, B.; Gillespie, D. Volume Exclusion in Calcium Selective Channels. *Biophys. J.* **2008**, *94* (9), 3486−3496.

(27) Kunz, W. *Specific Ion Effects*; World Scientific: Singapore, 2009; p 348.

(28) Kunz, W.; Neueder, R. An Attempt at an Overview. In *Specific Ion Effects*; Kunz, W., Ed.; World Scientific: Singapore, 2009; pp 11−54.

(29) Hünenberger, P.; Reif, M. *Single-Ion Solvation. Experimental and Theoretical Approaches to Elusive Thermodynamic Quantities*; Royal Society of Chemistry: London, 2011; p 690.

(30) Fraenkel, D. Monoprotic Mineral Acids Analyzed by the Smaller-Ion Shell Model of Strong Electrolyte Solutions. *J. Phys. Chem. B* **2010**, *115* (3), 557−568.

(31) Kontogeorgis, G. M.; Folas, G. K. *Thermodynamic Models for Industrial Applications: From Classical and Advanced Mixing Rules to Association Theories*; John Wiley & Sons: Chichester, U.K., 2009; p 721.

(32) Eisenberg, B.; Hyon, Y.; Liu, C. Energy Variational Analysis EnVarA of Ions in Water and Channels: Field Theory for Primitive Models of Complex Ionic Fluids. *J. Chem. Phys.* **2010**, *133*, 104104.

(33) Horng, T.-L.; Lin, T.-C.; Liu, C.; Eisenberg, B. PNP Equations with Steric Effects: A Model of Ion Flow through Channels. *J. Phys. Chem. B* **2012**, *116* (37), 11422−11441.

(34) Borukhov, I.; Andelman, D.; Orland, H. Adsorption of Large Ions from an Electrolyte Solution: a Modified Poisson−Boltzmann Equation. *Electrochim. Acta* **2000**, *46* (2−3), 221−229.

(35) Kornyshev, A. A. Double-Layer in Ionic Liquids: Paradigm Change? *J. Phys. Chem. B* **2007**, *111* (20), 5545−5557.

(36) Santangelo, C. D. Computing Counterion Densities at Intermediate Coupling. *Phys. Rev. E* **2006**, *73* (4), 041512.

(37) Bazant, M. Z.; Storey, B. D.; Kornyshev, A. A. Double Layer in Ionic Liquids: Overscreening Versus Crowding. *Phys. Rev. Lett.* **2011**, *106* (4), 046102.

(38) Gouy, M. Sur la Constitution de la Charge électrique à la surface d'un électrolyte. *J. Phys. (Paris)* **1910**, *9*, 457−468.

(39) Chapman, D. L. A Contribution to the Theory of Electrocapillarity. *Philos. Mag.* **1913**, *25*, 475−481.

(40) Warshel, A.; Russell, S. T. Calculations of Electrostatic interactions in Biological Systems and in Solutions. *Q. Rev. Biophys.* **1984**, *17*, 283−422.

(41) Davis, M. E.; McCammon, J. A. Electrostatics in Biomolecular Structure and Dynamics. *Chem. Rev.* **1990**, *90*, 509−521.

(42) Vlachy, V. Ionic Effects Beyond Poisson-Boltzmann Theory. *Annu. Rev. Phys. Chem.* **1999**, *50* (1), 145−165.

(43) Bazant, M. Z.; Kilic, M. S.; Storey, B. D.; Ajdari, A. Towards an Understanding of Induced-Charge Electrokinetics at Large Applied Voltages in Concentrated Solutions. *Adv. Colloid Interface Sci.* **2009**, *152* (1−2), 48−88.

(44) Eisenberg, B. Crowded Charges in Ion Channels. In *Advances in Chemical Physics*; Rice, S. A., Ed.; John Wiley & Sons, Inc.: New York, 2011; pp 77−223 (also on arXiv at http://arxiv.org/abs/1009.1786v1).

(45) Eisenberg, B. A Leading Role for Mathematics in the Study of Ionic Solutions. *SIAM News* **2012**, *45* (9), 11−12.

(46) Eisenberg, B. Life's Solutions. A Mathematical Challenge, 2012; available on arXiv as http://arxiv.org/abs/1207.4737.

(47) Fiedziuszko, S. J.; Hunter, I. C.; Itoh, T.; Kobayashi, Y.; Nishikawa, T.; Stitzer, S.; Wakino, K. Dielectric Materials, Devices, and Circuits. *IEEE Trans. Microwave Theory Tech.* **2002**, *50* (3), 706−720.

(48) Varsos, K.; Luntz, J.; Welsh, M.; Sarabandi, K. Electric Field-Shaping Microdevices for Manipulation of Collections of Microscale Objects. *Proc. IEEE* **2011**, *99* (12), 2112−2124.

(49) Fonseca, J.; Boda, D.; Nonner, W.; Eisenberg, B. Conductance and Concentration Relationship in a Reduced Model of the K+ Channel. *Biophys. J.* **2010**, *98*, 117a.

(50) Jadhao, V.; Solis, F. J.; de la Cruz, M. O. Simulation of Charged Systems in Heterogeneous Dielectric Media via a True Energy Functional. *Phys. Rev. Lett.* **2012**, *109* (22), 223905.

(51) Stern, O. Zur theorie der Elektrolytischen Doppleschicht. *Z. Elektrochem.* **1924**, *30*, 508−516.

(52) Borukhov, I.; Andelman, D.; Orland, H. Steric Effects in Electrolytes: A Modified Poisson-Boltzmann Equation. *Phys. Rev. Lett.* **1997**, *79* (3), 435.

(53) Storey, B. D.; Bazant, M. Z. Effects of Electrostatic Correlations on Electrokinetic Phenomena. *Phys. Rev. E: Stat., Nonlinear, Soft Matter Phys.* **2012**, *86* (5Pt 2), 056303.

(54) Wei, G.; Zheng, Q.; Chen, Z.; Xia, K. Variational Multiscale Models for Charge Transport. *SIAM Rev.* **2012**, *54* (4), 699−754.

(55) Liu, J.-L. Numerical Methods for the Poisson−Fermi Equation in Electrolytes. *J. Comput. Phys.* **2013**, *247* (0), 88−99.

(56) Vasileska, D.; Goodnick, S. M.; Klimeck, G. *Computational Electronics: Semiclassical and Quantum Device Modeling and Simulation*; CRC Press: New York, 2010; p 764.

(57) Eisenberg, B. Ions in Fluctuating Channels: Transistors Alive. *Fluctuation Noise Lett.* **2012**, *11* (01), 1240001 (available on arXiv.org with Paper ID arXiv:q-bio/0506016v3).

(58) Helfferich, F. *Ion Exchange (1995 reprint)*; McGraw Hill reprinted by Dover: New York, 1962; p 640.

(59) Buchner, R.; Barthel, J. Dielectric Relaxation in Solutions. *Annu. Rep. Prog. Chem., Sect. C: Phys. Chem.* **2001**, *97*, 349−382.

(60) Schutz, C. N.; Warshel, A. What are the Dielectric "constants" of Proteins and how to Validate Electrostatic Models? *Proteins* **2001**, *44* (4), 400−17.

(61) Ng, J.; Vora, T.; Krishnamurthy, V.; Chung, S.-H. Estimating the Dielectric Constant of the Channel Protein and Pore. *Eur. Biophys. J.* **2008**, *37* (2), 213−222.

12058

dx.doi.org/10.1021/jp408330f | *J. Phys. Chem. B* 2013, 117, 12051−12058